AGU PUBLICATIONS

Geophysical Research Letters

RESEARCH LETTER

10.1002/2015GL065091

Key Points:
- Seasonal sea level anomalies are affected by large-scale climate phenomena
- Dynamical models have skill in predicting seasonal sea level anomalies
- The dynamical model skill is larger than published statistical techniques

Supporting Information:
- Supporting Information S1

Correspondence to:
P. C. McIntosh,
peter.mcintosh@csiro.au

Citation:
McIntosh, P. C., J. A. Church, E. R. Miles, K. Ridgway, and C. M. Spillman (2015), Seasonal coastal sea level prediction using a dynamical model, *Geophys. Res. Lett.*, *42*, 6747–6753, doi:10.1002/2015GL065091.

Received 24 JUN 2015
Accepted 27 JUL 2015
Accepted article online 29 JUL 2015
Published online 22 AUG 2015

Seasonal coastal sea level prediction using a dynamical model

Peter C. McIntosh[1], John A. Church[1], Elaine R. Miles[2], Ken Ridgway[1], and Claire M. Spillman[2]

[1]CSIRO Oceans and Atmosphere Flagship, Hobart, Tasmania, Australia, [2]Bureau of Meteorology, Melbourne, Victoria, Australia

Abstract Sea level varies on a range of time scales from tidal to decadal and centennial change. To date, little attention has been focussed on the prediction of interannual sea level anomalies. Here we demonstrate that forecasts of *coastal* sea level anomalies from the dynamical Predictive Ocean Atmosphere Model for Australia (POAMA) have significant skill throughout the equatorial Pacific and along the eastern boundaries of the Pacific and Indian Oceans at lead times out to 8 months. POAMA forecasts for the western Pacific generally have greater skill than persistence, particularly at longer lead times. POAMA also has comparable or greater skill than previously published statistical forecasts from both a Markov model and canonical correlation analysis. Our results indicate the capability of physically based models to address the challenge of providing skillful forecasts of seasonal sea level fluctuations for coastal communities over a broad area and at a range of lead times.

1. Introduction

Many millions of people living in coastal regions are vulnerable to sea level extremes resulting from the combined effect of storm surges, seasonal and interannual sea level anomalies, and long-term sea level rise [*Nicholls and Cazenave*, 2010]. Accurate coastal sea level predictions would assist in preparing for extreme events. While sea level rise related to climate change is of overriding importance on multidecadal time scales, the variations on seasonal and shorter time scales are of immediate concern. Seasonal sea level anomalies in the region of interest can exceed 25 cm (Figures 1a and S1 in the supporting information), are comparable to the magnitude of nontidal anomalies, and are significantly correlated with the El Niño–Southern Oscillation (ENSO) [*Menéndez and Woodworth*, 2010]. As a result they can add significantly to storm surges or exacerbate the effects of low sea levels.

While sea level rise has been a major focus of international research [*Church et al.*, 2013], and there are a number of operational storm surge prediction programs, the influence and prediction of interannual and seasonal sea level anomalies has received less attention, with statistically based operational prediction schemes available at only a few locations in the western equatorial Pacific Ocean [*Chowdhury et al.*, 2014, 2007]. Local and regional seasonal-to-interannual sea level anomalies are strongly affected by large-scale climate phenomena and ocean dynamical processes that are central to the predictive skill of dynamical models such as Predictive Ocean Atmosphere Model for Australia (POAMA) and other dynamical models used for the prediction of interannual climate anomalies. The seasonal forecast skill of POAMA originates primarily from the ENSO coupled ocean-atmosphere interaction in the equatorial Pacific region [*Wang et al.*, 2011].

Miles et al. [2014] have evaluated the large-scale skill of POAMA sea level predictions. Here we extend that work to evaluate POAMA's skill to predict coastal sea level as measured by coastal and island tide gauges in the Pacific and eastern Indian Ocean.

2. Data and Methods

POAMA consists of a global coupled ocean-atmosphere dynamical model and an ensemble generation initialization scheme [*Hudson et al.*, 2013]. The ocean grid is relatively coarse, being 2° east-west, and increasing from 0.5° at the equator to 1.5° at the poles. There are 25 vertical levels, with 13 in the top 200 m. Forecasts are produced in real time, and a set of retrospective forecasts (hindcasts) extending back to 1981 is available for assessing model skill. Forecasts are typically of 1 month averages and extend for 9 months. Ocean initial conditions are generated by the POAMA Ensemble Ocean Data Assimilation System (PEODAS) [*Yin et al.*, 2011] using an approximate ensemble Kalman filter [*Oke et al.*, 2005]. While this system assimilates surface and

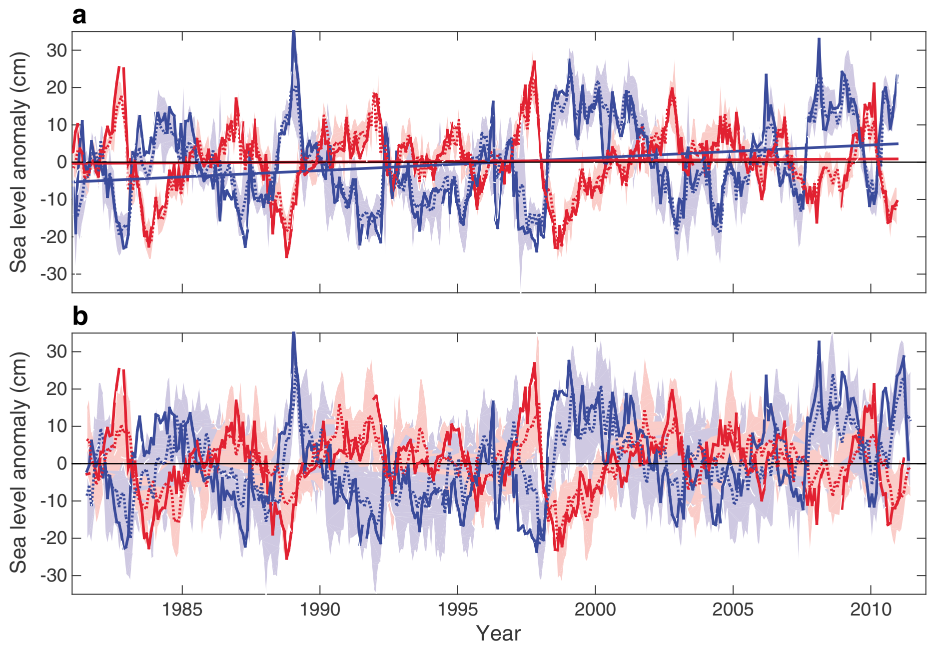

Figure 1. Observed (solid) and forecast (dashed) sea level anomalies at Malakal (blue) and Christmas Island (red) in the Pacific. Forecast lead times are (a) 0 month and (b) 6 months. The seasonal cycle has been removed, but the linear trend over 1981–2010 is retained and is shown in Figure 1a for both sites. The spread of the 33 ensemble members (5th–95th percentiles) is also shown (shading).

subsurface observations of temperature and salinity, it does not use in situ or satellite observations of sea level. POAMA has been shown to be skillful at predicting the ENSO signal in the Pacific at lead times up to 9 months [*Hudson et al.*, 2010], including the ability to predict some of the key inter-El Niño differences in the pattern of sea surface temperature anomalies [*Griesser and Spillman*, 2012; *Hendon et al.*, 2009]. In an earlier phase of this work, we have demonstrated that PEODAS and POAMA are able to represent large-scale seasonal sea level anomalies skillfully across the tropical Pacific and parts of the Indian Ocean with lead times exceeding 3 months [*Miles et al.*, 2014]. The lead time is defined by convention as the time between the start of the forecast and the beginning of the 1 month forecast period.

To evaluate POAMA's ability to forecast *coastal* mean sea level, we use monthly sea level data over the 30 year period 1981–2010 from a representative selection of tide gauge stations in the tropical Pacific Ocean and along the eastern boundaries of the Pacific and Indian Oceans (Figure 2a and Table S1 in the supporting information) obtained from the Permanent Service for Mean Sea Level [*Holgate et al.*, 2012] and the University of Hawaii Sea Level Center [*UHSLC*, 2014]. All tide gauge stations used here have long records with minimal gaps and provide a representative spatial coverage of the study region. Missing tide gauge observations are ignored rather than interpolated. Sea level on the POAMA grid is linearly interpolated to the tide gauge locations, unless the tide gauge is located outside the ocean model grid, in which case the nearest grid point is used.

The ocean dynamical processes associated with forecast skill are indicated schematically in Figure 2b. These will be discussed in the context of POAMA's skill at forecasting sea level (Figures 2c and 2e) compared to the skill at forecasting sea surface temperature (Figures 2d and 2f). The former is calculated using TOPEX/Poseidon and Jason-1 satellite data [*Miles et al.*, 2014], while the latter is assessed using the Hadley Centre's sea ice and sea surface temperature data set HadISST1 [*Rayner et al.*, 2003].

Skill is measured by the anomaly correlation coefficient (Pearson's "*r*") after linearly detrending the forecast and data and removing the seasonal cycle. Detrending prevents long time scale sea level changes from artificially increasing the correlation skill. Linear detrending is adequate for the relatively short 30 year period considered. When comparing two correlation coefficients, Fisher's *z* transformation [*Press et al.*, 1986] is used with 1 degree of freedom per year. Since our hypothesis is that our results are more skillful, a one-sided test is warranted. The time period representing 1 degree of freedom is calculated at each tide gauge station

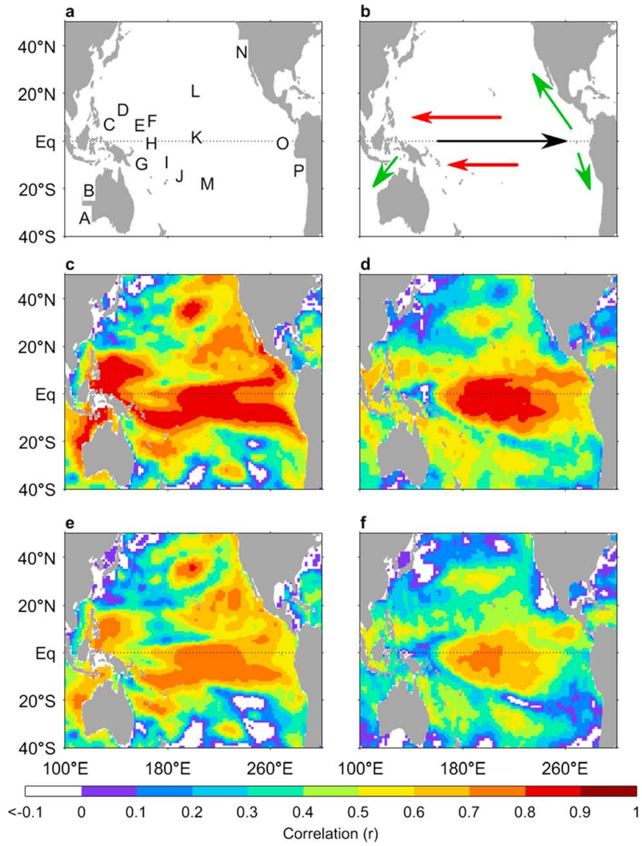

Figure 2. (a) Location of tide gauges (uppercase letters; see Table S1 in the supporting information for details); (b) arrows indicating the approximate Kelvin wave guides (black), Rossby wave paths (red), and coastally trapped waveguides (green). Correlation skill (*r*) of POAMA forecast of 1 month (c and e) sea level and (d and f) sea surface temperature forecasts compared to observed satellite sea levels and observed sea surface temperatures at lead times of 3 months (Figures 2c and 2d) and 6 months (Figures 2e and 2f), respectively, for all start months in the years for which satellite sea level data are available (1993–2010).

from the first zero crossing of the autocorrelation function and also from twice the *e*-folding time [*Leith*, 1973]. The average of all these values is 11.5 months.

The skill at forecasting individual tide gauge records is calculated as a function of lead time over all months (Figure 3). (Skill for individual months is available in Figure S2 in the supporting information.) The forecast period is for 1 month unless otherwise noted. For example, sea level forecasts for the month of April at lead times 0, 1, and 2 months would be initialized on 1 April, 1 March, and 1 February, respectively. Forecast skill is compared to the skill of a persistence forecast, that is, a forecast that sea level anomaly does not change from the initial value. In this case, a lead time zero forecast of April sea level would be the observed monthly mean sea level in March.

Model sea level anomalies are calibrated to remove known biases in the model mean and ensemble spread. The calibration is performed over 30 years separately for each lead time and for each start month to allow for seasonally dependent bias and model drift. The calibration method scales both the variance of the ensemble mean and the ensemble spread to match the observations. This ensures that the climatological variance of the forecasts is the same as that of the observations and that the mean square error of the ensemble mean equals the climatological average of the ensemble variance [*Johnson and Bowler*, 2009]. This differs from the method used by *Miles et al.* [2014] in that it not only removes the mean bias but also corrects the variance and ensemble spread. The calculation is cross validated by leaving out the year being calibrated. Calibration improves the statistical reliability of the forecasts by ensuring a realistic ensemble spread. In the absence of cross validation, calibration does not alter the correlation skill. The addition of cross validation reduces the forecast skill slightly.

3. Results

Examples of the observed and forecast monthly sea level anomalies at lead times of 0 and 6 months from the western and central/eastern Pacific (Malakal and Christmas Island, respectively) are shown in Figure 1. The opposite sign of the sea level anomalies at these two stations indicates the well-known oscillation of sea level across the Pacific [*Allan et al.*, 1996] associated with ENSO. The predictions for all locations are given in Figure S1 in the supporting information. The equatorial Kelvin and Rossby waveguides associated with this oscillation, as well as the coastally trapped waves propagating away from the equator along the west coasts of the Americas and Australia, are shown schematically in Figure 2b. The skill of POAMA, measured by the correlation between the ensemble mean sea level forecast and satellite altimeter data [*Miles et al.*, 2014], is greatest along these waveguides (Figures 2c and 2e). The skill typically exceeds 0.8 within 10° of the equator at lead 0 (not shown), decreasing at lead times of 3 and 6 months but generally remaining above 0.6 along the waveguides (Figures 2c and 2e).

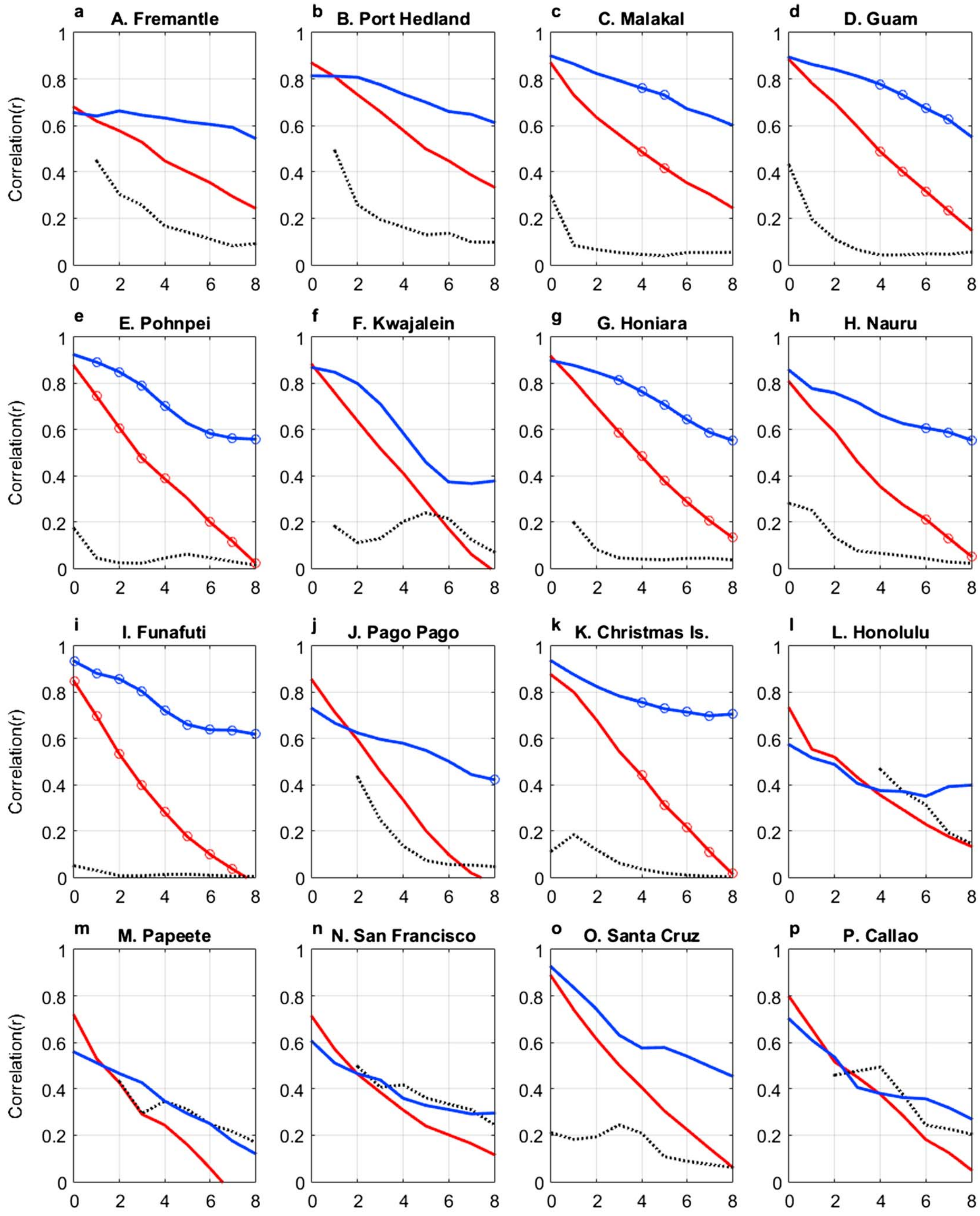

Figure 3. Correlation skill (r) between POAMA ensemble mean forecast and tide gauge observations (blue) and between a persistence forecast and observations (red) as a function of lead time for all months for 1981–2010. The black dashed line is the p value for the hypothesis that the POAMA correlation skill is greater than the skill of persistence. Circles indicate where POAMA skill is greater than persistence skill at the 95% significance level ($p = 0.05$).

POAMA sea level forecasts generally have greater skill than forecasts of sea surface temperature (compare Figure 2c with Figure 2d and Figure 2e with Figure 2f). POAMA's skill at forecasting the depth of the 20°C isotherm (a measure of thermocline depth) is very similar to its sea level skill in the equatorial Pacific (not shown). The dominant Kelvin and Rossby waves in the equatorial ocean have a direct relation between thermocline depth and sea level, while they have only an indirect relation to sea surface temperature [*Rebert et al.*, 1985]. These ocean dynamical wave processes are responsible for the relatively high skill of POAMA sea level forecasts.

At tide gauges in the western equatorial Pacific Ocean (15°S–15°N, west of 150°W), the POAMA forecast skill is high at zero lead time, exceeding 0.9 at most locations (Figures 3c–3k). The skill often exceeds the skill of persistence at the 95% significance level at lead times of up to 8 months, with the POAMA skill advantage increasing at longer lead times. A persistence forecast assumes no change from the initial condition and is a useful benchmark for ENSO-related seasonal forecasts [*Torrence and Webster*, 1998]. For example, at Guam (Figure 3d), the lead 0 skill of POAMA and persistence is the same, but after 3 months the skill of persistence decreases to 0.6, whereas POAMA takes 8 months for the skill to decrease to the same value. This represents a substantial increase in forecast lead time at a useful level of skill. We note the difficulty in establishing a high level of confidence (95%) in POAMA's improvement in skill due to the limited degrees of freedom typical of studies at interannual time scales. However, there is a degree of informal confidence to be gained from the widespread increase in correlation skill associated with an understanding of the physical mechanisms underlying this.

There is a moderately significant skill increase in the eastern Indian Ocean (Figures 3a and 3b), following the ocean waveguide (Figure 2b) through the Indonesian Archipelago and south along the west coast of Australia to Port Hedland and Fremantle [*Hendon and Wang*, 2009]. Following the equatorial Pacific waveguide east to Santa Cruz in the Galapagos Islands, the skill is high at zero lead (Figure 3o) and then decreases out to a lead time of 4 months (similar to the fall in skill with persistence). At longer lead times, the skill remains almost constant compared to a continuing fall in skill in persistence. A similar pattern is seen at the coast at Callao (Figure 3p). Along the North American west coast at San Francisco (Figure 3n), POAMA performs less well than persistence for small lead times but has larger skill for lead times greater than 3 months. The reason for the reduced model skill along the North and South American coasts may be the inability of POAMA to resolve sufficiently the local winds causing upwelling of cold water, and hence altered sea level, close to the coast. In addition, the combination of relatively sparse ocean observations and the coarse (2°) east-west grid of the ocean component of POAMA may not be capable of adequately initializing and propagating Kelvin waves along this coast.

Away from the equatorial waveguide in the central Pacific, POAMA shows comparatively lower skill at short lead times but maintains a useful advantage over persistence at longer lead times at Papeete (Figure 3m) and, to a lesser extent, at Honolulu (Figure 3l).

POAMA forecast skill shows a strong seasonal cycle at many of the tide gauge stations (Figure S2 in the supporting information). The Northern Hemisphere spring predictability barrier [*Torrence and Webster*, 1998] results in a reduction in skill at longer lead times for forecasts starting in March–May in the western North Pacific (Malakal, Pohnpei, and Kwajalein). However, in the South Pacific and east of the dateline, Funafuti, Pago Pago, and Papeete (Figures S2i, S2j, and S2m in the supporting information) have their greatest skill for forecasts starting in March to May. In the eastern Indian Ocean, and at the skillful stations in the eastern Pacific (Santa Cruz and Callao, Figures S2a, S2b, S2o, and S2p in the supporting information), the greatest skill is for forecasts starting between about November and February.

The spread of the ensemble of forecasts provides information about the uncertainty inherent in these forecasts, and it is desirable to provide predictions in a form that acknowledges this uncertainty (shaded area in Figures 1b and S1 in the supporting information). The simplest probabilistic forecast is to provide the chance of sea level exceeding the long-term median value. A measure of skill of such a forecast is the statistical reliability [*Wilks*, 2007], which assesses how accurately each level of chance is realized in the long term. For example, considering all forecasts that sea level has a 70% chance of exceeding the median, it is desirable that sea level was observed to exceed the median about 70% of the time. In general, we find that forecasts with higher correlations are also the most reliable (see Figure S3 in the supporting information). In practical terms, forecasts that have high correlations and are reliable will tend to have an ensemble spread that encompasses the observed sea level most of the time. For example, at Malakal and Christmas Island the observed sea level lies within the 90th percentile of the 6 month lead forecast ensemble 83% and 79% of the time, respectively (see Figure 1b). These figures would be exactly 90%, given the calibration method used, if the observed and modeled sea levels were exactly Gaussian and cross validation was not applied.

4. Discussion and Conclusions

Compared to the Markov model of *Xue and Leetmaa* [2000] (their Figures 4 and 5), the POAMA monthly forecast skill at Christmas Island and Malakal (also known as Koror) is greater at both sites for all lead times,

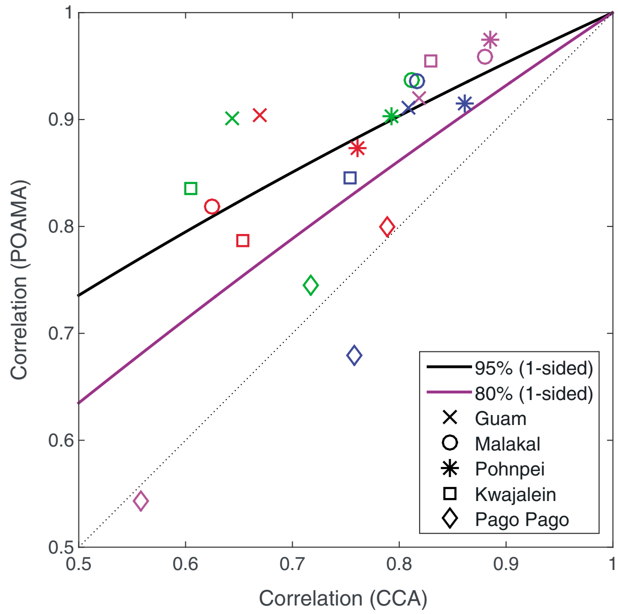

Figure 4. Correlation skill of POAMA compared to CCA [*Chowdhury et al.*, 2014] for zero month lead forecasts of 3-monthly seasonal sea level: April-May-June (red), July-August-September (green), OND (pink), and JFM (blue), at Guam, Malakal, Pohnpei, Kwajalein, and Pago Pago. The POAMA correlation is larger at the 95% significance level above the black line (one-sided test) and larger at the 80% significance level above the magenta line (one-sided test).

primarily due to a better representation of the 1982–1983 and 1997–1998 El Niño events and the 1988–1989 La Niña event. For example, the greatest improvement in skill is at Christmas Island at lead time zero, where the POAMA skill is 0.93 compared to the Markov model skill of 0.87 (significant at the 84% level for a one-sided test assuming 1 degree of freedom per year). At Malakal at lead 0, POAMA has a skill of 0.90 compared to the Markov model skill of 0.83 (one-sided significance of this increase is 80%). At lead times of 3 and 6 months, POAMA is only slightly more skillful than the Markov model, although in both cases POAMA represents the 1988–1989 La Niña event more accurately.

POAMA seasonal forecast skill also generally exceeds that of an operational sea level forecasting scheme for a set of U.S.-affiliated Pacific Islands (Guam, Malakal, Pohnpei, Kwajalein, and Pago Pago) using canonical correlation analysis (CCA) based on sea surface temperature [*Chowdhury et al.*, 2007] and now also surface winds [*Chowdhury et al.*, 2014] (Figure 4). POAMA forecasts of seasonal (3 month) sea level at lead 0 have a higher correlation than the CCA method at five sites and in all seasons except for October, November, and December (OND) and January, February, and March (JFM) at Pago Pago. Twelve (out of 20) of the POAMA correlations are significantly greater than those of the CCA method at the 95% level, with a further four significantly greater at the 80% level. While the addition of surface winds to the statistical CCA method has resulted in an increase in skill, it is clear that modeling a broader range of dynamical features using POAMA leads to further improvements in skill. A dynamical model-based approach also enhances the ability to diagnose the physical processes underpinning forecast skill, providing a basis for further improvement. Importantly, POAMA does not assume climate stationarity, so the model should remain applicable under a changing climate.

These POAMA results combined with a previous global assessment study [*Miles et al.*, 2014] demonstrate the skill of a dynamical model at predicting seasonal coastal sea level anomalies. The region of maximum skill is located near the equator in the Pacific, and along the waveguides emanating from this region (Figure 2), with small variations zonally and larger variations meridionally. However, there is considerable scope for further improvement. A large component of the POAMA skill is derived from its ability to predict ENSO accurately, and the skill is smaller outside the waveguides extending from the Pacific equatorial region. Refinement of the relatively coarse model grid will help to resolve more accurately the islands in the Western Pacific, the narrow upwelling regions in the eastern Pacific, and the western boundary regions. Higher resolution will also help improve the atmospheric winds that are an important component of the key coupled ocean-atmosphere dynamical processes. Finally, improved initial conditions through explicit use of altimeter data should help initialize the large-scale ocean waves more accurately.

The 30 year time series of observed and forecasted sea level at almost all sites show multiyear to decadal oscillations with amplitudes of 50 cm or more (Figures 1 and S1 in the supporting information). It is encouraging that POAMA appears capable of representing these longer time scales, and this is attributed to the ability of the initialization scheme to assimilate ocean and atmospheric observations prior to each forecast.

The present results demonstrate the potential skill of an operational dynamical seasonal forecast system for predicting coastal sea level anomalies up to 8 months in advance. Such seasonal sea level predictions would allow coastal communities to better prepare for and manage the impacts of severe coastal flooding and erosion associated with high sea levels [*Committee on Sea Level Rise in California Oregon and Washington et al.*, 2012], as well as the impacts of low sea levels such as coral mortality and Taimasa (foul-smelling tide in Samoa [*Pirhalla et al.*, 2011]). These results also serve to demonstrate that while sea level rise of up to 1 m this century is a significant concern, the greatest impact will come from a combination of the rapid sea level fluctuations of half this amplitude that are already occurring on much shorter time scales superimposed on the ongoing rise. The ability to predict significant sea level variations with a lead time of several months is likely to have immediate value and utility. Seasonal sea level predictions and knowledge of the risk from storm surges combined with projections of sea level rise and changes in seasonal variability would significantly advance the development of informed management plans to increase the resilience of coastal communities.

Acknowledgments
POAMA model output was obtained from the Australian Bureau of Meteorology (http://poama.bom.gov.au/data_server.shtml). Tide gauge observations were obtained from the Permanent Service for Mean Sea Level (http://www.psmsl.org/data/obtaining/) and the University of Hawaii Sea Level Center (http://uhslc.soest.hawaii.edu/data/download/fd). TOPEX/Poseidon and Jason-1 data were obtained from the NASA Physical Oceanography Distributed Active Archive Center (https://data.nasa.gov/). Jason-2/OSTM data were obtained from AVISO (http://www.aviso.altimetry.fr/en/data.html). HadISST1 sea surface temperature data were obtained from the Hadley Centre, UK Meteorological Office (http://www.metoffice.gov.uk/hadobs/hadisst/). This research contributes to the Pacific Australia Climate Change Science and Adaptation Program (PACCSAP) funded by AusAID and the Australian Department of Climate Change and Energy Efficiency and delivered by the Australian Bureau of Meteorology and CSIRO. We thank Andrew Marshall, Xuebin Zhang, and Harry Hendon for critically reading the earlier versions of the manuscript.

The Editor thanks two anonymous reviewers for their assistance in evaluating this paper.

References

Allan, R., J. Lindesay, and D. Parker (1996), *El Niño Southern Oscillation and Climatic Variability*, 405 pp., CSIRO, Collingwood, Australia.

Chowdhury, M. R., P.-S. Chu, T. Schroeder, and N. Colasacco (2007), Seasonal sea-level forecasts by canonical correlation analysis—An operational scheme for the U.S.-affiliated Pacific Islands, *Int. J. Climatol.*, *27*(10), 1389–1402.

Chowdhury, M. R., P. S. Chu, and C. C. Guard (2014), An improved sea level forecasting scheme for hazards management in the US-affiliated Pacific Islands, *Int. J. Climatol.*, *34*(7), 2320–2329.

Church, J. A., et al. (2013), Sea level change, in *Climate Change 2013: The Physical Science Basis. Contribution of Working Group I to the Fifth Assessment Report of the Intergovernmental Panel on Climate Change*, edited by T. F. Stocker et al., pp. 1137–1216, Cambridge Univ. Press, Cambridge, U. K., and New York.

Committee on Sea Level Rise in California Oregon and Washington, Board on Earth Sciences and Resources (BESR), Ocean Studies Board (OSB), Division on Earth and Life Studies (DELS), and National Research Council (2012), *Sea-Level Rise for the Coasts of California, Oregon, and Washington: Past, Present, and Future*, The National Academies Press, Washington, D. C.

Griesser, A. G., and C. M. Spillman (2012), SST forecast skill of the new intra-seasonal configuration of POAMA-2, *CAWCR Res. Lett.*, *8*, 10–16.

Hendon, H. H., and G. Wang (2009), Seasonal prediction of the Leeuwin Current using the POAMA dynamical seasonal forecast model, *Clim. Dyn.*, *34*(7–8), 1129–1137.

Hendon, H. H., E. Lim, G. Wang, O. Alves, and D. Hudson (2009), Prospects for predicting two flavors of El Niño, *Geophys. Res. Lett.*, *36*, L19713, doi:10.1029/2009GL040100.

Holgate, S. J., A. Matthews, P. L. Woodworth, L. J. Rickards, M. E. Tamisiea, E. Bradshaw, P. R. Foden, K. M. Gordon, S. Jevrejeva, and J. Pugh (2012), New data systems and products at the Permanent Service for Mean Sea Level, *J. Coastal Res.*, *29*(3), 493–504.

Hudson, D., O. Alves, H. H. Hendon, and G. Wang (2010), The impact of atmospheric initialisation on seasonal prediction of tropical Pacific SST, *Clim. Dyn.*, *36*(5–6), 1155–1171.

Hudson, D., A. G. Marshall, Y. Yin, O. Alves, and H. H. Hendon (2013), Improving intraseasonal prediction with a new ensemble generation strategy, *Mon. Weather Rev.*, *141*(12), 4429–4449.

Johnson, C., and N. Bowler (2009), On the Reliability and Calibration of Ensemble Forecasts, *Mon. Weather Rev.*, *137*(5), 1717–1720.

Leith, C. (1973), The standard error of time-average estimates of climatic means, *J. Appl. Meteorol.*, *12*(6), 1066–1069.

Menéndez, M., and P. L. Woodworth (2010), Changes in extreme high water levels based on a quasi-global tide-gauge data set, *J. Geophys. Res.*, *115*, C10011, doi:10.1029/2009JC005997.

Miles, E. R., C. M. Spillman, J. A. Church, and P. C. McIntosh (2014), Seasonal prediction of global sea level anomalies using an ocean–atmosphere dynamical model, *Clim. Dyn.*, *43*, 2131–2145.

Nicholls, R. J., and A. Cazenave (2010), Sea-level rise and its impact on coastal zones, *Science*, *328*(5985), 1517–1520.

Oke, P. R., A. Schiller, D. A. Griffin, and G. B. Brassington (2005), Ensemble data assimilation for an eddy-resolving ocean model of the Australian region, *Q. J. R. Meteorol. Soc.*, *131*(613), 3301–3311.

Pirhalla, D., V. Ransi, M. S. Kendall, and D. Fenner (2011), Chapter 2 – Oceanography of the Samoan Archipelago, in *Biogeographic Assessment of the Samoan Archipelago, NOAA Tech. Memo. NOS NCCOS*, vol. 132 edited by M. S. Kendall and M. Poti, 229 pp., Silver Spring, Md.

Press, W. H., B. P. Flannery, S. A. Teukolsky, and W. T. Vetterling (1986), *Numerical Recipes: The Art of Scientific Computing*, 818 pp., Cambridge Univ. Press, Cambridge.

Rayner, N. A., D. E. Parker, E. B. Horton, C. K. Folland, L. V. Alexander, D. P. Rowell, E. C. Kent, and A. Kaplan (2003), Global analyses of sea surface temperature, sea ice, and night marine air temperature since the late nineteenth century, *J. Geophys. Res.*, *108*(D14), 4407, doi:10.1029/2002JD002670.

Rebert, J. P., J. R. Donguy, G. Eldin, and K. Wyrtki (1985), Relations between sea level, thermocline depth, heat content, and dynamic height in the tropical Pacific Ocean, *J. Geophys. Res.*, *90*(C6), 11,719–11,725, doi:10.1029/JC090iC06p11719.

Torrence, C., and P. J. Webster (1998), The annual cycle of persistence in the El Niño/Southern Oscillation, *Q. J. R. Meteorol. Soc.*, *124*(550), 1985–2004.

UHSLC (2014), University of Hawaii Sea Level Center. [Available at http://uhslc.soest.hawaii.edu.]

Wang, G., D. Hudson, Y. Yin, O. Alves, H. Hendon, S. Langford, G. Liu, and F. Tseitkin (2011), POAMA-2 SST skill assessment and beyond, *CAWCR Res. Lett.*, *6*, 40–46.

Wilks, D. S. (2007), *Statistical Methods in the Atmospheric Sciences*, 627 pp., Academic Press, Inc., San Diego, Calif.

Xue, Y., and A. Leetmaa (2000), Forecasts of tropical Pacific SST and sea level using a Markov model, *Geophys. Res. Lett.*, *27*(17), 2701–2704, doi:10.1029/1999GL011107.

Yin, Y., O. Alves, and P. R. Oke (2011), An ensemble ocean data assimilation system for seasonal prediction, *Mon. Weather Rev.*, *139*(3), 786–808.